

See discussions, stats, and author profiles for this publication at: <https://www.researchgate.net/publication/282224660>

Silver Diffusion in Organic Optoelectronic Devices: Deposition Related Processes vs. SIMS Analysis Artefacts

ARTICLE *in* THE JOURNAL OF PHYSICAL CHEMISTRY C · SEPTEMBER 2015

Impact Factor: 4.77 · DOI: 10.1021/acs.jpcc.5b06860

READS

35

4 AUTHORS, INCLUDING:



Patrick Philipp

Luxembourg Institute of Science and Technol...

43 PUBLICATIONS **196** CITATIONS

SEE PROFILE



John Kieffer

University of Michigan

138 PUBLICATIONS **1,442** CITATIONS

SEE PROFILE



Tom Wirtz

Luxembourg Institute of Science and Technol...

94 PUBLICATIONS **579** CITATIONS

SEE PROFILE

Silver Diffusion in Organic Optoelectronic Devices: Deposition-Related Processes versus Secondary Ion Mass Spectrometry Analysis Artifacts

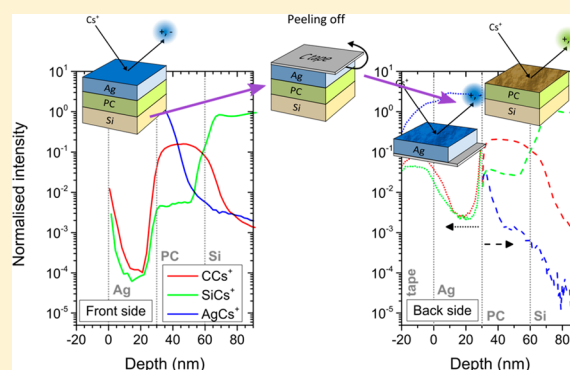
Patrick Philipp,^{*,†} Khanh Q. Ngo,[†] John Kieffer,[‡] and Tom Wirtz[†]

[†]Advanced Instrumentation for Ion Nano-Analytics (AINA), MRT Department, Luxembourg Institute of Science and Technology, 41 rue du Brill, L-4422 Belvaux, Luxembourg

[‡]Department of Materials Science and Engineering, University of Michigan, Ann Arbor, Michigan 48109-2136, United States

S Supporting Information

ABSTRACT: The development of organic optoelectronic devices relies on controlling interfaces during thin-film deposition and requires an accurate characterization of the film composition at these interfaces. Dynamic secondary ion mass spectrometry (SIMS) is widely used to investigate multilayer thin-film structures. Routine analysis protocols are well established for classical semiconductor samples, but for organic or mixed metallic–organic samples the limitations of the technique are less well established. In the current work, low-energy dynamic SIMS is used on metal–organic multilayered model structures similar to those in organic optoelectronic devices to study the origin of diffusion of metal into the organic layer (e.g., irradiation-induced diffusion during SIMS analysis or during the deposition process). Samples contain silver and organic compounds sequentially deposited by thermal evaporation in vacuum onto a Si substrate. They are analyzed using a 250 eV to 1 keV Cs⁺ primary ion beam. It is found that the mixing of silver into the organic layer depends on the impact energy and the conditions for sample preparation. This irradiation effect can be minimized by a back-side depth profiling approach, which was developed in this work. By applying this method, it is shown that some silver is likely to diffuse into the organic layers during the deposition process.



INTRODUCTION

Molecular-level dimensional control is imperative for the fabrication of multilayered structures found in organic optoelectronic devices (e.g., organic light-emitting diodes, organic photovoltaic cells, etc.).¹ At the same time, various deposition conditions and combination of different materials can result in uneven or poorly defined interfaces and different morphologies.^{2–4} A detailed knowledge of interface morphologies and the layer composition can be used to improve the deposition processes and the device properties.⁵

Secondary ion mass spectrometry (SIMS) has proven to be a valuable tool for the characterization of interfaces for semiconductor and metallic samples.^{6,7} Depth profiling of organic samples is by far less developed. A major issue is the loss of information about the organic structure due to the fragmentation of molecules under classical analysis conditions, i.e., kiloelectronvolt monatomic primary ions. Reduced fragmentation is achieved most easily by cluster ion bombardment.^{8,9} For depth profiling applications, large cluster beams have been shown to be most successful. Studies made with C₆₀⁺ cluster beams on alternating layers of Irganox1010 and Irganox3114 achieved a depth resolution of at best 2.5 nm. The depth resolution is limited by roughness formation at the

crater bottom.¹⁰ Massive argon cluster ion beams lead to an even more reduced fragmentation, but the depth resolution that has been obtained up to now is about 6 nm for a multilayered sample of Irganox1010 and Irganox3114¹¹ and approximately 12 and 8.5 nm for C₆₀/SnPc bilayers on silicon.¹² For organic optoelectronic devices, cluster ion bombardment is not the only possibility for depth profiling. Under low-energy Cs⁺ bombardment, the fragmentation is less prevalent than for kiloelectron-volt bombardment,^{13,14} and stable secondary ion intensities of small characteristic fragments are obtained under steady-state conditions.¹⁵ The successful depth profiling of metal–organic multilayered samples¹⁶ and the ability to extract information on the interface morphology¹⁷ have been reported previously. This includes the control of roughness formation for the experimental conditions used^{18,19} and of Cs–O nanodot formation in the areas irradiated by a Cs⁺ primary ion beam²⁰ due to the high mobility of cesium.²¹

Depth profiles presented in previous work also show high Ag secondary ion intensities inside the organic layer.^{16,17} Other

Received: July 16, 2015

Revised: September 24, 2015

authors have already encountered this problem. Fostiropoulos et al. investigated the metal diffusion into organic films by SIMS by comparing the depth profiles from an Ag/Mg/CuPc:C₆₀ device with and without lifting off the Ag/Mg cathode.²² The sample without cathode shows a clear Mg diffusion into the organic layer due to deposition-induced diffusion. At the same time, a high Mg intensity is seen across the entire device. This is attributed to sputter-induced diffusion of the metal during SIMS analysis. Song et al. investigated the Ag/Alq₃ interface of samples using dynamic SIMS²³ and X-ray photoelectron spectroscopy (XPS).²⁴ Diffusion of silver into the organic layer is observed using SIMS and XPS depth profiles. However, in both studies the origin of the silver diffusion is not clarified.

The issue of irradiation-induced diffusion is not limited to organic semiconductor samples, but it has been known for a long time in the semiconductor industry. The problem can be circumvented by characterizing the front side of an interface by a regular SIMS depth profiling and the back side of the same interface by a depth profile carried out from the back side of the sample.²⁵ However, this requires careful sample preparation. After some silicon is deposited on the sample surface and most of the initial substrate is removed from the back side until getting close to the interface of interest, the newly prepared surface for the back-side depth profile needs to be parallel to all interfaces and to the initial sample surface.^{26,27} This technique has been applied to various systems, including Ge/Pd ohmic contacts on InP,²⁸ the segregation of boron toward the silicon surface,²⁹ and the characterization of HfO₂^{30,31} and HfSiO₂³⁰ thin films. This work is still ongoing for the current generation of devices in which it is applied to high-mobility III–V channel materials.³²

In the present work, the origin of the diffusion of metal species into the organic layer as well as the influence of sample properties on these mechanisms is investigated in order to develop reliable protocols for the characterization of multi-layered metal–organic devices. The silver diffusion has been studied for various sample compositions, for films deposited at two different temperatures, and for different impact energies during SIMS depth profiling. A back-side depth profiling approach is also investigated.

■ EXPERIMENTAL SECTION

Sample Preparation. For this study, samples were prepared with a silver layer and an organic layer deposited on top of a silicon substrate. The samples were prepared by vacuum thermal evaporation at room temperature and at -60 °C. The organic layers contain aluminum tris(8-hydroxyquinoline) (C₂₇H₁₈N₃O₃Al, named Alq₃) or phthalocyanine derivatives (C₃₂H₁₆N₈M, where M is a metal, named MPc). The evaporation was carried out at a pressure of approximately 10^{-6} mbar using a commercial deposition system (Angstrom Engineering AMod). The silicon substrates were cleaned by sonicating in detergent, acetone, trichloroethylene, and isopropanol. During the deposition process, the film thickness was monitored using a quartz crystal microbalance, which was precalibrated using ellipsometry measurements. For each sample, the silver layer and the organic layer had the same thickness of 30 nm. For the SIMS depth profiles, the time scale was converted into a depth scale using the film thicknesses determined during the deposition process. The samples are described in Table 1.

SIMS Analyses. SIMS experiments were carried out on a CAMECA Sc-Ultra instrument. The influence of the impact

Table 1. List of Samples and Preparation Conditions^a

name	sample	deposition temperature
Alq ₃	Ag/Alq ₃ /Si	room temperature
Pc	Ag/Pc/Si	room temperature
FePc	Ag/FePc/Si	room temperature
ZnPc	Ag/ZnPc/Si	room temperature
CuPc_RT	Ag/CuPc/Si	room temperature
CuPc_CS	Ag/CuPc/Si	-60 °C

^aAll layers have a thickness of 30 nm.

energy on irradiation-induced diffusion was studied for 250 eV, 500 eV, and 1 keV in the negative secondary ion mode. For 250 eV, the sample voltage was set to -2 keV, and for 500 eV and 1 keV to -3 keV. This leads to incidence angles of 38° , 47° , and 51° with respect to the surface normal, respectively. Depth profiles for the studies on substrate temperature during the deposition process and back-side analysis were carried out at 500 eV in both secondary ion modes. Incidence angles correspond to 47° for the negative and 64° for the positive secondary ion mode. For all analyses, the primary ion current was changed between 3 and 20 nA and the mass resolution $M/\delta M$ was set to 400. The contrast aperture was set to $300\ \mu\text{m}$, and the energy slit was closed to a width of 45 eV. The raster size was fixed to $300 \times 300\ \mu\text{m}^2$, and the field of view was set to a diameter of $100\ \mu\text{m}$.

To study the diffusion of the metal into the organic layer during the deposition process, a peel-off method was used to characterize the metal/organic interface and to carry out back-side SIMS depth profiles. A schematic of the process is shown in Figure 1. An adhesive tape is put on the sample surface. After

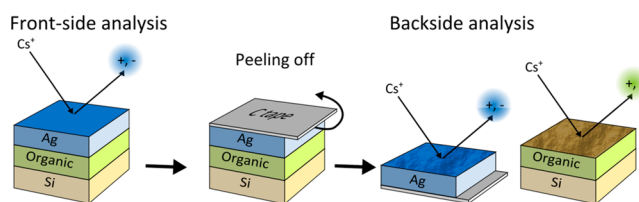


Figure 1. Schematic showing front-side and back-side analyses.

the tape is peeled off, it is generally expected that the Ag and organic layers stick to the tape and no organic molecules remain on the silicon substrate. However, for the Alq₃ and Pc samples, only the silver layer peels off and the organic layer remains on the silicon substrate. Hence, both sides of the interface are now directly accessible for ablation by the primary ion beam, as shown in Figure 1.

Afterward, all samples are depth profiled using SIMS. The characterization of the original sample is called front-side analysis, and the characterizations of the Ag layer of the peeled-off samples starting from the metal–organic interface and, separately, of the organic layer remaining on the silicon substrate are called back-side analysis. The back-side analysis should reveal the real distribution of silver in the organic layer.

■ RESULTS AND DISCUSSION

Influence of Sample Composition and Impact Energy on Diffusion. The best way to choose secondary ion fragments was discussed in previous papers.^{15,17} In short, characteristic fragments producing high secondary ion intensities are selected and their intensities are observed both

in the negative and positive secondary ion mode for different sample compositions, different preparation conditions, and as a function of the primary ion impact energy. In this section, the diffusion of silver into the metal–organic samples during SIMS depth profiling is investigated from the front side.

To study the influence of sample composition on silver diffusion, the best results have been obtained in the positive MCs^+ mode; hence, only these results are shown (Figure 2).

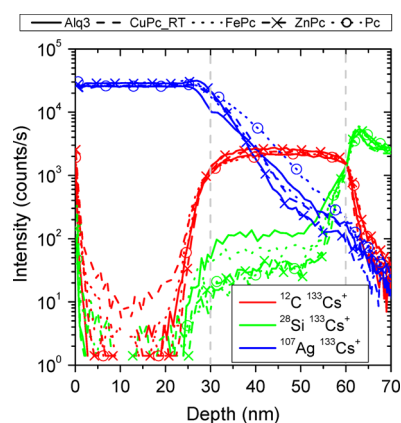


Figure 2. Positive MCs^+ secondary ion intensities as a function of depth at 500 eV Cs^+ bombardment for the samples Alq_3 , CuPc_RT , FePc , ZnPc , and Pc . The depth profiles are normalized with respect to the Cs^+ intensities.

After normalization with respect to the Cs^+ intensity, the intensity of AgCs^+ , CCs^+ , and SiCs^+ are identical for the different samples in the silver layers, organic layers, and silicon substrate, respectively. The difference in molecular composition is so small that the CCs^+ intensities in the different organic layers are similar for all samples. In addition, the AgCs^+ intensity decreases only slowly in the organic layers (Figure 2), which indicates that silver enters into the organic layer by diffusion rather than by atomic mixing. Diffusion here refers to diffusion of silver into the organic layer during the deposition process while the atomic mixing occurs during SIMS depth profiling. The interface widths at the Ag/organic and organic/Si interfaces are larger in the positive mode than in the negative mode (cf. Figure S1 in the Supporting Information). Thus, the Ag diffusion is at least partially due to sputter-induced diffusion. Differences between the two modes are probably also due to the distinct incidence angles of 47° (negative mode) and 64° (positive mode), which lead to different atomic mixing. This aspect will be discussed in more detail later. In addition to what is shown in the literature,^{22–24} our results reveal that the irradiation-induced silver diffusion does not change significantly with the organic molecules of the deposited layer, but more with the secondary ion mode. Different secondary ion formation mechanisms lead to various matrix effects,³³ and an influence of the impact angle on the sputter-induced diffusion for a given energy cannot be excluded.

Panels a and b of Figure 3 show the influence of the impact energies on silver diffusion for the Alq_3 and CuPc_RT samples, respectively. For comparison purposes, the depth profiles at the different impact energies are normalized with respect to the Si^- intensity in the Si substrate at 2×10^7 counts/s. For the Alq_3 sample, the Ag^- intensity in the Ag layer does not change with impact energy. However, the CN^- intensity at 1 keV is slightly higher than at 500 and 250 eV. This is partially due to changing

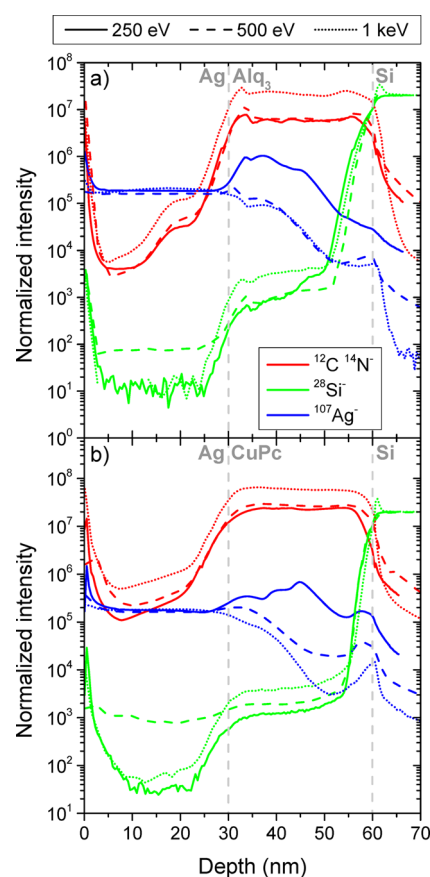


Figure 3. Normalized secondary ion intensities as a function of depth at different impact energies: (a) sample Alq_3 and (b) sample CuPc_RT . The depth profiles are normalized with respect to the bulk Si^- intensity.

sputter rates; the sputter rate in the organic layer decreases faster than the one in the inorganic layers. Variations due to changing transmission of the mass spectrometer with the different voltage settings are removed by normalization. The Ag^- depth profiles at 1 keV and 500 eV are similar. However, when the impact energy is reduced to 250 eV, the Ag^- signal increases when entering the Alq_3 layer, which is not observed for the other energies. Inside the organic layer, the Ag^- intensity is about 1 order of magnitude higher than at 500 eV and 1 keV. The increase is too sizable to be accounted for only as a result of an increased ionization probability due to a higher Cs surface concentration. Hence, sputter-induced diffusion must be a major contribution. A possible effect of the Cs concentration on Ag^- should also be visible when comparing the 1 keV and 500 eV energies, but these profiles are almost identical inside the organic layer.

For sample CuPc_RT , the trends seen in the different depth profiles are similar to those of sample Alq_3 ; after normalization, the CN^- intensity is slightly higher at 1 keV than at 500 and 250 eV. In addition, the Ag^- intensity in the Ag layers is always the same. At 250 eV, the same intensity increases strongly in the organic layer, but not for the other energies. There are also small differences between the Ag^- depth profiles at 500 eV and 1 keV. For our experiments, the 1 keV depth profile shows the lowest amount of Ag diffusion. The intensity of mass interferences at mass $m/z = 107$ in the organic layer is less than 2×10^3 counts/s (when the Ag^- intensities are between 2×10^4 and 2×10^5 counts/s at the CuPc/Si interface), so that

the major contribution to $m/z = 107$ is due to Ag diffusion. The intensity of mass interferences was measured in a bulk CuPc layer without any silver layer above. Close to the Ag/organic and organic/Si interfaces, the variation in Ag secondary ion intensity as a function of impact energy is probably caused by matrix effects. Major differences inside the layer are due to increased diffusion at lower impact energies, especially at 250 eV. The influence of the different incident angles, which are 38° at 250 eV, 47° at 500 eV, and 51° at 1 keV, is not clear.

To conclude, the diffusion of Ag into the organic layer is seen at all impact energies, and it is most pronounced at 250 eV in the negative secondary ion mode. Hence, to limit the diffusion during sputtering, the impact energy during depth profiling on the Cameca SC-Ultra instrument must not be too low. When the current results are combined with the conditions for the highest depth resolution from a previous paper,¹⁷ the 500 eV or 1 keV impact energies give the best results for depth profiling of organic multilayered samples for optoelectronic applications, depending on the organic layer. On Alq₃, 500 eV and 1 keV give a similar mixing of silver into the organic layer, but the highest interface resolution is obtained when using the 500 eV impact energy. On CuPc, the mixing of silver into the organic layer is lowest at 1 keV.

Influence of Substrate Temperature during Sample Preparation. Figure 4 shows the depth profiles of the

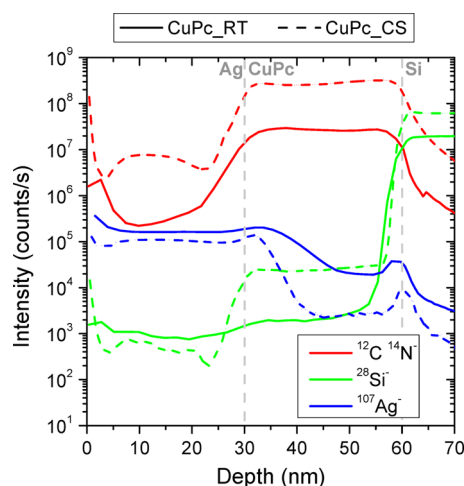


Figure 4. Negative secondary ion intensities as a function of depth for samples CuPc_RT and CuPc_CS analyzed at 500 eV.

CuPc_RT sample prepared at room temperature and the CuPc_CS sample prepared using a cooling substrate. Both samples have the same layer thicknesses, but sample CuPc_CS exhibits half the interface width compared to sample CuPc_RT (3.2 and 1.8 nm for sample CuPc_CS and 5.9 and 2.9 nm for sample CuPc_RT at the Ag/organic and organic/Si interfaces, respectively). The interface width is taken between 16% and 84% of the layer intensity. Diffusion of Ag into the organic layer is present for both samples, but is less pronounced in CuPc_CS than in CuPc_RT. Although sample CuPc_CS has a higher Si⁻ intensity in the Si substrate and a higher CN⁻ intensity in the organic layer, it is the Ag⁻ intensity in the CuPc film that is about 1 order of magnitude lower than in CuPc_RT. Based on the experimental deposition conditions, the CuPc layer should have the same α -phase structure in both samples, as described in ref 34. Nevertheless, their morphologies are different. For the low-temperature substrate, the CuPc layer has finer grains.

When the substrate temperature increases, the crystals grow larger.^{34,35} This change in morphology produces films with different densities and surface roughness.³⁶ As a result, not only does the sample prepared using the low substrate temperature have a sharper interface but also diffusion is suppressed because of the higher density of silver, which is consistent with the SIMS depth profiles.

For sample CuPc_CS, the intensity of Ag⁻ decreases to $\sim 2 \times 10^3$ counts/s at about 13 nm from the Ag/CuPc interface. This corresponds to the intensity due to mass interferences at $m/z = 107$ in the CuPc mass spectrum. Therefore, Ag diffusion in the CuPc_CS sample may stop at a depth of about 13 nm from the Ag/CuPc interface. Conversely, Ag diffusion in sample CuPc_RT prepared at room temperature seems to go beyond 17 nm from the Ag/CuPc interface and possibly reaches until the CuPc/Si interface. The peaks in Ag⁻ depth profiles observed at the CuPc/Si interface in both samples are caused by a matrix effect coming from the native silicon oxide.³⁷

Back-Side SIMS Depth Profiling. In this section, we compare depth profiles from front-side and back-side analysis for the Alq₃ and Pc samples to get further insights into the diffusion mechanisms. The results are shown for the negative and positive secondary ion modes at 500 eV and 1 keV.

As mentioned in the Experimental Section, the organic layer stayed on the silicon substrate after the peel-off process. The adhesion of silver layers on organic films has already been investigated by other authors. Using photoemission spectroscopy and X-ray photoelectron spectroscopy for the characterization of metal–organic interfaces, many authors demonstrated that silver does not react with the organic layer,^{38–40} while there are strong chemical interactions between aluminum and organic molecules.^{41,42} Hence, depending on the metallic layer, either the silver/organic or the organic/silicon interface exhibits the weaker bonding, and either the silver layer comes off alone or all three layers are removed by the tape. This was also shown by Jin et al.³⁶

In Figure 5 we compare front-side and back-side analyses for sample Alq₃. Upon combining the depth profiles from the adhesive tape and the Si substrate with organic layer to a total depth profile, and comparing it to the front-side analysis, it is obvious that the Ag/Alq₃/Si system separates at the Ag/Alq₃ interface. The Ag layer sticks to its entirety to the tape and the Alq₃ layer to the Si substrate. The depth profiles from the

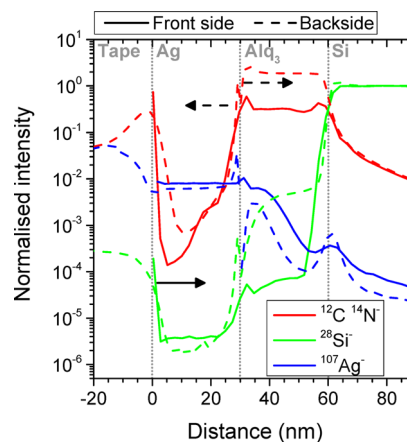


Figure 5. Negative secondary ion intensities from the analyses of the front side, the peeled-off sample, and the back side of the Ag layer for sample Alq₃ at 500 eV.

peeled-off layer on the carbon tape show a stable intensity of Ag^- and a decrease of secondary ion intensities at $m/z = 26$ (CN^-) and $m/z = 28$ (Si^-) as a function of sputtering time (Figure 5). The decrease of C- and N-containing ion intensities shows that some organic molecules or contaminations stick to the Ag layer after peel-off. The intensity of $m/z = 28$ in the organic layer comes from carbon, nitrogen, and oxygen containing mass interferences with the silicon signal. In the material remaining on the substrate, the Ag^- intensity is high at the beginning of the organic layer, although peeling the Ag layer off reduced the Ag^- intensity in the organic layer. Either some Ag stayed on the organic layer during the peel-off or Ag diffused inside the organic layer during the deposition process.

Additional information is obtained by carrying out the same experiments in the positive secondary ion mode. For the depth profiles in the positive mode (Figure 6), the AgCs^+ intensity in

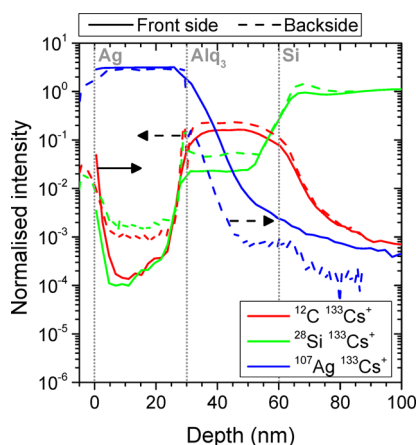


Figure 6. Positive MCs^+ secondary ion intensities from the analyses of the front side, the peeled-off sample, and the back side of the Ag layer for sample Alq_3 at 1 keV.

the peeled-off sample decreases faster than the Ag^- intensity for the negative mode. In addition, by using the MCs^+ secondary ions, the cusp in the Ag^- depth profile at the interfaces, which is due to the matrix effect caused by air contact and native silicon oxide, is suppressed.^{33,43,44} Furthermore, the higher AgCs^+ intensity in the front-side analysis than in the back-side analysis provides evidence for irradiation-induced diffusion during front-side depth profiling (Figure 6). The MCs^+ ions are less influenced by the matrix effect, showing clearly that the positive secondary ion mode is suited better to studying the influence of irradiation-induced diffusion than the negative mode.

Back-side depth profiling in SIMS removes most of the artifacts related to irradiation-induced diffusion, and it is the only method that can provide reliable information on the interfaces. Yet, it is not clear if the remaining silver in the organic film seen in the back-side depth profiles is diffusing during the deposition process or if it is due to atomic mixing. To clarify this point, the decaying AgCs^+ intensity (Figure 6) is fitted to (a) the solution of Fick's law which describes diffusion processes, and which was already used in other studies to describe diffusion in similar molecules⁴⁵

$$c(x, t) = c_0 \operatorname{erfc}\left(\frac{x - x_0}{2\sqrt{Dt}}\right) \quad (1)$$

where c is the concentration, c_0 the concentration at time 0, and D the diffusion coefficient, and (b) the SIMS response function⁶

$$c(x) = c_0 e^{-(x-x_0)/\lambda} \quad (2)$$

where λ is the decay length. This procedure can be applied only when no matrix effect is present, i.e., it is limited to the MCs^+ mode. The decaying AgCs^+ signal is fitted best by the diffusion function (Figure 7), which reproduces the AgCs^+ intensities for

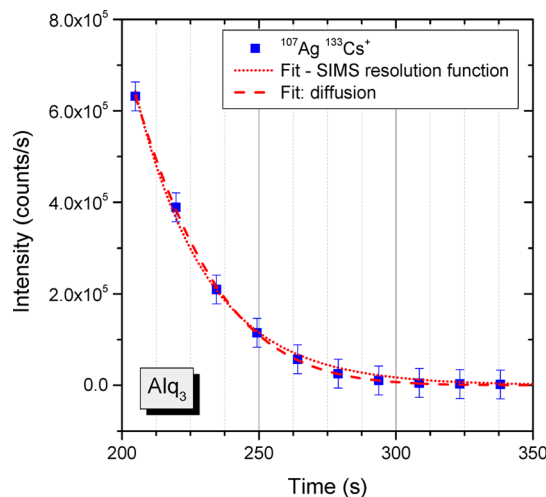


Figure 7. Decay of the AgCs^+ signal in the Si layer of the Alq_3 sample fitted by the SIMS resolution and the erfc function.

the whole depth profile. The parameters obtained by the diffusion fit are $c_0 = 2.25 \times 10^6 \pm 0.58 \times 10^6$ cts/s, $x_0 = 150.42 \pm 11.49$ nm, $2(Dt)^{1/2} = 71.45 \pm 4.47$ nm⁻¹, and $R^2 = 0.9997$. It should be noted that the time scale in Figure 7 corresponds to the time of sputtering during the SIMS depth profile and that it is not related to the onset of silver diffusion.

Parameters for the fit for the SIMS resolution function are $c_0 = 2.25 \times 10^6$ cts/s, $x_0 = 171.97 \pm 1.28$ nm, $\lambda = 26.28 \pm 0.80$ nm⁻¹, and $R^2 = 0.9969$. In order for the SIMS resolution fit to converge, one parameter needed to be fixed, and c_0 was chosen as 2.25×10^6 cts/s, i.e., the same value as for the diffusion fit. This gave a good result. For this fit, the situation is slightly different than for the SIMS resolution function. It produces a faster decay at high intensity and overlays only partially with the AgCs^+ data. However, the fitting must be interpreted with care. When considering the error bars, both fits manage to reproduce the experimental data points, with the difference that the trend of the data points is better described by the diffusion function. Hence, this suggests that the silver seen in the back-side depth profile is probably diffusing during the deposition process into the organic layer. Irradiation-induced diffusion during SIMS depth profiling is another diffusion process which cannot be excluded and which would probably produce a similar profile. Getting the real silver distribution in the sample requires the organic layer to stick to the silver during the peeling-off and realizing a back-side depth profiling through the organic and silver layer. Nevertheless, the peel-off as carried out in this work allowed for a significant reduction of the irradiation-induced silver diffusion as seen during front-side SIMS depth profiling.

When peeling off the Pc sample, the layers separate at a position similar to that for the Alq_3 sample, with the Ag layer sticking to the carbon tape and the organic layer staying on the

Si substrate. However, in the negative mode the Ag^- depth profile in the substrate after peeling off shows almost no presence of Ag on or in the organic layer (Figure 8). The

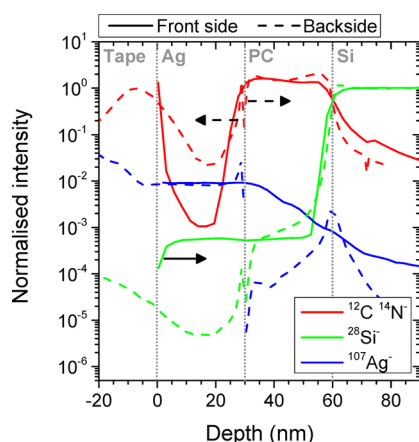


Figure 8. Negative secondary ion intensities from the analyses of the front side, the peeled-off sample, and the back side of the Ag layer for sample Pc at 500 eV.

normalized intensity of Ag^- is about 10^{-4} counts/s in the organic layer after peel-off but varies in the range from 10^{-2} to 10^{-4} counts/s in the front-side analysis. The value of 10^{-4} normalized counts/s corresponds to the mass interference at $m/z = 107$ from the organic material. It has been measured in a thick Pc film, which was not covered by a layer of silver. Similar to sample Alq_3 , some residual Ag is seen on the organic layer in the positive secondary ion mode. The CsAg^+ intensity in the organic layer where Ag has been peeled-off is about 2 orders of magnitude lower than for the front-side analysis, i.e., it varies from 2×10^{-2} to 10^{-5} counts/s in the organic layer after peeling off and from 2×10^0 to 10^{-3} counts/s in the front-side analysis (Figure 9). Thus, the back-side depth profiling removes successfully the effect of radiation-induced diffusion and shows that the entire silver layer has been peeled off.

Moreover, in the Pc sample, sputter-induced diffusion is identified in both negative and positive mode. Ag seems to stick less well to Pc than to Alq_3 , so that it could be removed almost completely by the peeling off process. Intensities in the pre-

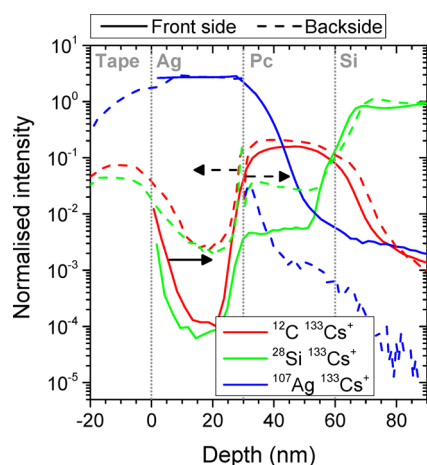


Figure 9. Positive MCs^+ secondary ion intensities from the analyses of the front side, the peeled-off sample, and the back side of the Ag layer for sample Pc at 1 keV.

equilibrium regime are increased by contaminations adsorbing on the surface after the peeling off, but they are not related to Ag diffusion. In general, conclusive results for any organic layer could be obtained when peeling off metal and organic layers, but this would require studying different systems, i.e., using aluminum as metal layer, or developing a more sophisticated method for sample preparation.

CONCLUSIONS

SIMS depth profiling of multilayered metal–organic samples are often not easy to interpret because of irradiation-induced diffusion processes and matrix effects. In this work, experimental conditions were optimized to obtain reliable data. In general, 500 eV and 1 keV Cs^+ bombardment combined with the MC_x^+ mode produce the lowest matrix effects and irradiation-induced diffusion. These conditions are successful in comparing different organic layers and studying the effect of sample temperature during the deposition process on interface properties.

In addition, a method for back-side SIMS depth profiling was developed by peeling off the silver layer. Ideally, both the silver and organic layer should have been removed; however, because of a better adhesion of the organic molecules on silicon than silver on organic molecules, only the silver layer could be removed. However, the removal of the silver layer allows us to show that the Ag^- intensity in the organic layer is to a large extent due to the irradiation-induced diffusion of silver during the SIMS depth profiles. Minor diffusion of silver during the deposition process has been identified by back-side depth profiling.

ASSOCIATED CONTENT

Supporting Information

The Supporting Information is available free of charge on the ACS Publications website at DOI: 10.1021/acs.jpcc.5b06860.

Negative secondary ion intensities as a function of depth at 500 eV Cs^+ bombardment (PDF)

AUTHOR INFORMATION

Corresponding Author

*E-mail: patrick.philipp@list.lu.

Notes

The authors declare no competing financial interest.

ACKNOWLEDGMENTS

The present project was supported by the National Research Fund, Luxembourg (NSF-FNR-MAT-07-01) and the US National Science Foundation (NSF-DMR 0806867). We thank Yansha Jin, Samanthule Nola, and other students in Max Shtein's group at Michigan University for support in sample preparation. We thank Patrick Grysan from LIST for help with the AFM measurements.

REFERENCES

- (1) Krebs, F. C. *Stability and Degradation of Organic and Polymer Solar Cells*; John Wiley & Sons, Ltd: Chichester, 2012.
- (2) Berger, O.; Fischer, W. J.; Adolphi, B.; Tierbach, S.; Melev, V.; Schreiber, J. Studies on Phase Transformations of Cu-Phthalocyanine Thin Films. *J. Mater. Sci.: Mater. Electron.* **2000**, *11*, 331–346.
- (3) Yang, F.; Shtein, M.; Forrest, S. R. Morphology Control and Material Mixing by High-Temperature Organic Vapor-Phase Deposi-

tion and its Application to Thin-Film Solar Cells. *J. Appl. Phys.* **2005**, *98*, 014906.

(4) Lee, Y. L.; Tsai, W. C.; Maa, J. R. Effects of Substrate Temperature on the Film Characteristics and Gas-Sensing Properties of Copper Phthalocyanine Films. *Appl. Surf. Sci.* **2001**, *173*, 352–361.

(5) Grossiord, N.; Kroon, J. M.; Andriessen, R.; Blom, P. W. M. Degradation Mechanisms in Organic Photovoltaic Devices. *Org. Electron.* **2012**, *13*, 432–456.

(6) Dowsett, M. G.; Barlow, R. D. Characterization of Sharp Interfaces and Delta Doped Layers in Semiconductors Using Secondary Ion Mass Spectrometry. *Anal. Chim. Acta* **1994**, *297*, 253–275.

(7) Zalm, P. C. Ultra Shallow Doping Profiling with SIMS. *Rep. Prog. Phys.* **1995**, *58*, 1321–1374.

(8) Mahoney, C. M. Cluster Secondary Ion Mass Spectrometry of Polymers and Related Materials. *Mass Spectrom. Rev.* **2010**, *29*, 247–293.

(9) Fletcher, J. S.; Lockyer, N. P.; Vickerman, J. C. Developments in Molecular SIMS Depth Profiling and 3D Imaging of Biological Systems Using Polyatomic Primary Ions. *Mass Spectrom. Rev.* **2011**, *30*, 142–174.

(10) Shard, A. G.; Green, F. M.; Brewer, P. J.; Seah, M. P.; Gilmore, I. S. Quantitative Molecular Depth Profiling of Organic Delta-Layers by C60 Ion Sputtering and SIMS. *J. Phys. Chem. B* **2008**, *112*, 2596–2605.

(11) Lee, J. L. S.; Ninomiya, S.; Matsuo, J.; Gilmore, I. S.; Seah, M. P.; Shard, A. G. Organic Depth Profiling of a Nanostructured Delta Layer Reference Material Using Large Argon Cluster Ions. *Anal. Chem.* **2010**, *82*, 98–105.

(12) Mouhib, T.; Poleunis, C.; Möllers, R.; Niehuis, E.; Defrance, P.; Bertrand, P.; Delcorte, A. Organic Depth Profiling of C60 and C60/Phthalocyanine Layers Using Argon Clusters. *Surf. Interface Anal.* **2013**, *45*, 163–166.

(13) Mine, N.; Douhard, B.; Brison, J.; Houssiau, L. Molecular Depth-Profiling of Polycarbonate with Low-Energy Cs⁺ Ions. *Rapid Commun. Mass Spectrom.* **2007**, *21*, 2680–2684.

(14) Houssiau, L.; Douhard, B.; Mine, N. Molecular Depth Profiling of Polymers with Very Low Energy Ions. *Appl. Surf. Sci.* **2008**, *255*, 970–972.

(15) Ngo, K. Q.; Philipp, P.; Jin, Y.; Morris, S. E.; Shtein, M.; Kieffer, J.; Wirtz, T. Analysis and Fragmentation of Organic Samples by (Low-Energy) Dynamic SIMS. *Surf. Interface Anal.* **2011**, *43*, 88–91.

(16) Ngo, K. Q.; Philipp, P.; Jin, Y.; Morris, S. E.; Shtein, M.; Kieffer, J.; Wirtz, T. Analysis of Organic Multilayered Samples for Optoelectronic Devices by (Low-Energy) Dynamic SIMS. *Surf. Interface Anal.* **2011**, *43*, 194–197.

(17) Philipp, P.; Ngo, Q. K.; Shtein, M.; Kieffer, J.; Wirtz, T. Ag-Organic Layered Samples for Optoelectronic Applications: Interface Width and Roughening Using a 500 eV Cs⁺ Probe in Dynamic Secondary Ion Mass Spectrometry. *Anal. Chem.* **2013**, *85*, 381–388.

(18) Mansilla, C.; Philipp, P.; Wirtz, T. Roughening of Silicon (100) Surface During Low Energy Cs⁺ Ion Bombardment. *Nucl. Instrum. Methods Phys. Res., Sect. B* **2011**, *269*, 905–908.

(19) Mansilla, C.; Philipp, P.; Wirtz, T. Roughness Formation in (100) Silicon During Low-Energy Cs⁺ Bombardment. *Surf. Interface Anal.* **2013**, *45*, 97–100.

(20) Ngo, K. Q.; Philipp, P.; Kieffer, J.; Wirtz, T. Cs Oxide Aggregation in SIMS Craters in Organic Samples for Optoelectronic Application. *Surf. Sci.* **2012**, *606*, 1244–1251.

(21) Barry, P. R.; Philipp, P.; Wirtz, T. Structural Conditions for Cesium Migration to Si(100) Surface Employing Electronic Structure Calculations. *J. Phys. Chem. C* **2014**, *118*, 3443–3450.

(22) Fostiropoulos, K.; Rusu, M. Engineering of Hybrid Interfaces in Organic Photovoltaic Devices. *Sol. Energy Mater. Sol. Cells* **2011**, *95*, 1489–1494.

(23) Song, W.; Li, Z.; So, S. K.; Qiu, Y.; Zhu, Y.; Cao, L. Dynamic SIMS Characterization of Interface Structure of Ag/Alq₃/NPB/ITO Model Devices. *Surf. Interface Anal.* **2001**, *32*, 102–105.

(24) Song, W.; So, S. K.; Moulder, J.; Qiu, Y.; Zhu, Y.; Cao, L. Study on the Interaction Between Ag and Tris(8-hydroxyquinoline) Aluminum Using X-Ray Photoelectron Spectroscopy. *Surf. Interface Anal.* **2001**, *32*, 70–73.

(25) Shappirio, J. R.; Lareau, R. T.; Lux, R. A.; Finnegan, J. J.; Smith, D. D.; Heath, L. S.; Taysinglara, M. Metal Penetration and Dopant Redistribution Beneath Alloyed Ohmic Contacts to N-GaAs. *J. Vac. Sci. Technol., A* **1987**, *5*, 1503–1507.

(26) Ronsheim, P.; Chidambarrao, D.; Jagannathan, B.; Hunt, D. Backside Sputter Depth Profiling of Phosphorus Diffusion from a Polysilicon Source. *J. Vac. Sci. Technol., B: Microelectron. Process. Phenom.* **2002**, *20*, 448–450.

(27) Yeo, K. L.; Wee, A. T. S.; Liu, R.; NG, C. M.; See, A. SIMS Backside Depth Profiling of Ultrashallow Implants Using Silicon-on-Insulator Substrates. *Surf. Interface Anal.* **2002**, *33*, 373–375.

(28) Schwarz, S. A.; Pudensi, M. A. A.; Sands, T.; Gmitter, T. J.; Bhat, R.; Koza, M.; Wang, L. C.; Lau, S. S. Backside Secondary Ion Mass-Spectrometry Study of a Ge/Pd Ohmic Contact to InP. *Appl. Phys. Lett.* **1992**, *60*, 1123–1125.

(29) Shima, A.; Jinbo, T.; Natsuaki, N.; Ushio, J.; Oh, J. H.; Ono, K.; Oshima, M. A Model for the Segregation and Pileup of Boron at the SiO₂/Si Interface During the Formation of Ultrashallow p(+) Junctions. *J. Appl. Phys.* **2001**, *89*, 3458–3463.

(30) Nieveen, W.; Schueler, B. W.; Goodman, G.; Schnabel, P.; Moskito, J.; Mowat, I.; Chao, G. Analysis of High-k HfO₂ and HfSiO₄ Dielectric Films. *Appl. Surf. Sci.* **2004**, *231–232*, 556–560.

(31) Jiang, Z. X.; Kim, K.; Lerma, J.; Sieloff, D.; Tseng, H.; Hegde, R. I.; Luo, T. Y.; Yang, J. Y.; Triyoso, D. H.; Tobin, P. J. Characterization of HfO₂ Dielectric Films with Low Energy SIMS. *Appl. Surf. Sci.* **2006**, *252*, 7172–7175.

(32) Hopstaken, M. J. P.; Pfeiffer, D.; Copel, M.; Gordon, M. S.; Ando, T.; Narayanan, V.; Jagannathan, H.; Molis, S.; Wahl, J. A.; Bu, H.; et al. J. Physical Characterization of sub-32-nm Semiconductor Materials and Processes Using Advanced Ion Beam Based Analytical Techniques. *Surf. Interface Anal.* **2013**, *45*, 338–344.

(33) Gao, Y.; Marie, Y.; Saldi, F.; Migeon, H. N. On the SIMS Depth Profiling Analysis: Reduction of Matrix Effect. *Int. J. Mass Spectrom. Ion Processes* **1995**, *143*, 11–18.

(34) Yang, F.; Shtein, M.; Forrest, S. R. Morphology Control and Material Mixing by High-Temperature Organic Vapor-Phase Deposition and its Application to Thin-Film Solar Cells. *J. Appl. Phys.* **2005**, *98*, 014906.

(35) Lee, Y. L.; Tsai, W. C.; Maa, J. R. Effects of Substrate Temperature on the Film Characteristics and Gas-Sensing Properties of Copper Phthalocyanine Films. *Appl. Surf. Sci.* **2001**, *173*, 352–361.

(36) Jin, Y.; Yadav, A.; Sun, K.; Sun, H.; Pipe, K. P.; Shtein, M. Thermal Boundary Resistance of Copper Phthalocyanine-Metal Interface. *Appl. Phys. Lett.* **2011**, *98*, 093305.

(37) Williams, P.; Evans, C. A. Anomalous Enhancement of Negative Sputtered Ion Emission by Oxygen. *Surf. Sci.* **1978**, *78*, 324–338.

(38) Molodtsova, O. V.; Aristov, V.; Zhilin, V.; Ossipyan, Y.; Vyalikh, D. V.; Doyle, B.; Nannarone, S.; Knupfer, M. Silver on Copper Phthalocyanine: Abrupt and Inert Interfaces. *Appl. Surf. Sci.* **2007**, *254*, 99–102.

(39) Turak, A.; Grozea, D.; Feng, X. D.; Lu, Z. H.; Aziz, H.; Hor, A. M. Metal/Alq₃ Interface Structures. *Appl. Phys. Lett.* **2002**, *81*, 766–768.

(40) Song, W. J.; So, S. K.; Moulder, J.; Qiu, Y.; Zhu, Y. F.; Cao, L. L. Study on the Interaction Between Ag and Tris(8-hydroxyquinoline) Aluminum Using X-Ray Photoelectron Spectroscopy. *Surf. Interface Anal.* **2001**, *32*, 70–73.

(41) Isomura, N.; Mitsuoka, T.; Ohwaki, T.; Taga, Y. Chemical Structure of Aluminum/8-Hydroxyquinoline Aluminum Interface. *Jpn. J. Appl. Phys., Part 2* **2000**, *39*, L312–L314.

(42) Nguyen, T. P.; Ip, J.; Jolinat, P.; Destruel, P. XPS and Sputtering Study of the Alq₃/Electrode Interfaces in Organic Light Emitting Diodes. *Appl. Surf. Sci.* **2001**, *172*, 75–83.

(43) Gao, Y. A New Secondary Ion Mass Spectrometry Technique for III-V Semiconductor Compounds Using the Molecular Ions CsM⁺. *J. Appl. Phys.* **1988**, *64* (7), 3760–3762.

(44) Bock, W.; Gnaser, H.; Oechsner, H. Secondary Neutral and Secondary Ion Mass Spectrometry Analysis of TiN-Based Hard Coatings: an Assessment of Quantification Procedures. *Anal. Chim. Acta* **1994**, *297*, 277–283.

(45) Ju, Y. H.; Hsieh, C.; Liu, C. J. The Surface Reaction and Diffusion of NO₂ in Lead Phthalocyanine Thin Film. *Thin Solid Films* **1999**, *342*, 238–243.